Heteroleptic Copper Switches

Sanaz Kabehie,[†,‡] Mei Xue,[‡,§] Adam Z. Stieg,[‡,||] Monty Liong,[†,‡] Kang L. Wang,[§,||] and Jeffrey I. Zink*,[†,‡]

Department of Chemistry and Biochemistry, California NanoSystems Institute, and Device Research Laboratory, Department of Electrical Engineering, University of California, Los Angeles, California 90095, United States, and WPI Center for Materials Nanoarchitectonics (MANA), National Institute for Materials Science, Tsukuba, Japan

Received May 14, 2010; E-mail: zink@chem.ucla.edu

Abstract: Heteroleptic copper compounds have been designed and synthesized on solid supports. Chemical redox agents were used to change the oxidation state of the SiO_2-immobilized heteroleptic copper compounds from Cu(I) to Cu(II) and then back to Cu(I). Optical spectroscopy of a dimethyl sulfoxide suspension demonstrated the reversibility of the Cu(I)/Cu(II) SiO_2-immobilized compounds by monitoring the metal-to-ligand charge transfer peak at about 450 nm. Electron paramagnetic resonance spectroscopy was used to monitor the isomerization of Cu(I) tetrahedral to Cu(II) square planar. This conformational change corresponds to a 90° rotation of one ligand with respect to the other. Conductive atomic force microscopy and macroscopic gold electrodes were used to study the electrical properties of a p^+ Si-immobilized heteroleptic copper compound where switching between the Cu(I)/Cu(II) states occurred at −0.8 and +2.3 V.

Introduction

State variables represent a class of essential components in the emerging field of nanoelectronic devices[1−6] that serve as the physical representations of information used in memory and logic applications.[7] Important properties include switching speed, on/off ratio, maximum spatial density, limiting scaling factor, and on/off modulation method. Boolean logic remains the most commonly used information processing methodology in current technology and is based on two discrete states, represented by 1 or 0. A critical first step toward the fabrication of functional nanodevices capable of carrying out Boolean computation is the realization of a physical unit within the device that resides in two stable, distinguishable states. Subsequent integration of this nanostructure into the process of Si-based fabrication technology represents the crucial second step.

Rotational conformational states of transition-metal-containing compounds constitute state variables for which information storage relies on physical changes of the molecule. In particular,

transition metals offer useful features due to the accessibility of multiple oxidation states (low power consumption). Changes in transition metals include coordination number, color, and geometry.[8] Of specific interest here, metal complexes of copper[9−18] and nickel[19] are known to exhibit oxidation-state-dependent geometries. These distinct molecular conformations have potential to be employed as a state variable where the oxidation state of the metal center is used to drive conformational motion such as intramolecular rotation. For example, Cu(I) bis-1,10-phenanthroline compounds are tetrahedral, while Cu(II) analogues are square planar (Scheme 1). Similarly, the unique carbons in Ni(III) bis-dicarbollide cages adopt a transoid geometry with respect to one another, while Ni(IV) analogues

[†] Department of Chemistry and Biochemistry, University of California, Los Angeles.
[‡] California NanoSystems Institute, University of California, Los Angeles.
[§] Department of Electrical Engineering, University of California, Los Angeles.
[||] WPI Center for Materials Nanoarchitectonics.

(1) Balzani, V. C., A.; Venturi, M. *Molecular Devices and Machines—A Journey into the Nano World*, 2nd ed.; Wiley: Weinheim, 2006.
(2) Likharev, K. K. *J. Nanoelectron. Optoelectron.* **2008**, *3*, 203–230.
(3) Lu, W.; Lieber, C. M. *Nat. Mater.* **2007**, *6*, 841–850.
(4) Pischel, U. *Aust. J. Chem.* **2010**, *63*, 148–164.
(5) Silvi, S.; Venturi, M.; Credi, A. *J. Mater. Chem.* **2009**, *19*, 2279–2294.
(6) Kay, E. R.; Leigh, D. A.; Zerbetto, F. *Angew. Chem., Int. Ed.* **2007**, *46*, 72–191.
(7) Galatsis, K.; Khitun, A.; Ostroumov, R.; Wang, K. L.; Dichtel, W. R.; Plummer, E.; Stoddart, J. F.; Zink, J. I.; Jae Young, L.; Ya-Hong, X.; Ki Wook, K. *IEEE Trans. Nanotech.* **2009**, *8*, 66–75.
(8) Cotton, F. A. *Advanced Inorganic Chemistry*, 6th ed.; Wiley: New York, 1999.
(9) Chen, L. X.; Shaw, G. B.; Novozhilova, I.; Liu, T.; Jennings, G.; Attenkofer, K.; Meyer, G. J.; Coppens, P. *J. Am. Chem. Soc.* **2003**, *125*, 7022–7034.
(10) Miller, M. T.; Gantzel, P. K.; Karpishin, T. B. *Inorg. Chem.* **1998**, *37*, 2285–2290.
(11) Ruthkosky, M.; Kelly, C. A.; Castellano, F. N.; Meyer, G. J. *Coord. Chem. Rev.* **1998**, *171*, 309–322.
(12) Wang, X.; Lv, C.; Koyama, M.; Kubo, M.; Miyamoto, A. *J. Organomet. Chem.* **2005**, *690*, 187–192.
(13) Wang, X.; Lv, C.; Koyama, M.; Kubo, M.; Miyamoto, A. *J. Organomet. Chem.* **2006**, *691*, 551–556.
(14) Wang, X.; Wang, W.; Koyama, M.; Kubo, M.; Miyamoto, A. *J. Photochem. Photobiol. A: Chem.* **2006**, *179*, 149–155.
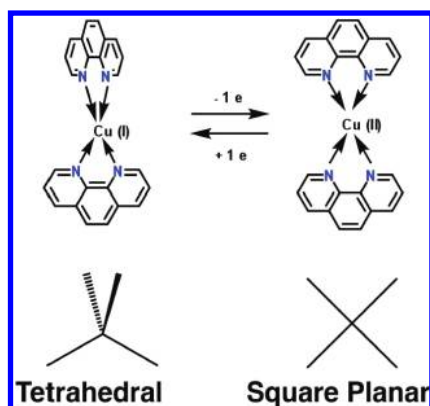(15) He, S.; Dennis, A. E.; Smith, R. C. *Macromol. Rapid Commun.* **2009**, *30*, 2079–2083.
(16) Colasson, B. X.; Dietrich-Buchecker, C.; Jimenez-Molero, M. C.; Sauvage, J.-P. *J. Phys. Org. Chem.* **2002**, *15*, 476–483.
(17) Collin, J. P.; Gavina, P.; Heitz, V.; Sauvage, J.-P. *New J. Chem.* **1997**, *21*, 525.
(18) Sauvage, J.-P. *Acc. Chem. Res.* **1998**, *31*, 611–619.
(19) Hawthorne, M. F.; Zink, J. I.; Skelton, J. M.; Bayer, M. J.; Liu, C.; Livshits, E.; Baer, R.; Neuhauser, D. *Science* **2004**, *303*, 1849–1851.

adopt a cisoid geometry.[20] Such isomerizations can thus be used as a state variable based on a redox-induced intra-rotational conformational change. Integration of nickel bis-dicarbollides onto a solid silicon support and solid-state switching of these systems have yet to be reported. The most highly developed nanoelectrical applications involve organic rotaxanes in a cross bar architecture.[21–24]

Silicon-immobilized heteroleptic copper compounds provide an attractive option as potential physical state variables due to their discrete rotational mechanical movement and robust integration with the Si surface. This one-electron redox-induced conformational change is reversible and occurs via the +1 and +2 oxidation states of copper, which isomerizes from tetrahedral to square planar geometries, respectively (Scheme 1). The redox potential of the copper switch constitutes the minimum energy required for information storage i.e., one electron per molecule at the voltage at which the redox event occurs. Because information storage is based on the nanoscopic movement of atomic nuclei about the copper center, the switching speed is on the order of the relevant rotational vibrational mode of the molecule.[9,25] Molecular integration onto a solid support necessitates a heteroleptic design (a metal center with two different ligands) whereby one ligand serves to immobilize the compound while the second ligand is able to move freely. In this way, a high-density layer of molecular switches can be immobilized onto a bottom electrode (i.e., p$^+$-doped Si) and sandwiched by a top electrode (i.e., macroscopic gold electrodes or a conductive AFM (cAFM) tip) to achieve state variable functionality.[25,26]

In this work, the design and synthesis of a family of Si-immobilized heteroleptic copper compounds is presented. The systems shown undergo reversible, intramolecular conformational motion upon a one-electron oxidation or reduction and represent a physical state variable toward applications in nanoscale logic and memory devices.[25,26] This system is particularly attractive due to its relatively low energetic activation barrier (−0.8 and +2.3 V) and potential for high spatial density. Switching between discrete conformation states occurs on the picosecond time scale,[9,25] and the molecules can be readily integrated into a silicon or silica solid-state platform.[25,26] A modular synthetic approach (Scheme 2) enables versatility in the design of size, shape, and function within the nanoarchitecture of these functionally engineered materials.

Results and Discussion

Heteroleptic copper compounds in solution undergo fast ligand exchange reactions between copper and bidentate ligands.[36,37] Although pure homoleptic copper compounds have been isolated, pure heteroleptic copper compounds in the solid state are less common.[38] The first reported mixed-ligand copper systems, HETPHEN (*het*eroleptic bis(*phen*anthroline))[39,40] were synthesized via thermodynamic control. An approach used in the past employs bulky aryl substituents at the 2,9- and 4,7-bis(imine) coordination sites, where steric bulk and electronic effects selectively control the metal complexation equilibrium through $\pi-\pi$ stacking interactions.[41] In the reported solution studies, steric and electronic factors governing the selective HETPHEN principles were observed by ^{1}H NMR and ESI-MS titrations.[42] Although strategic for locked positions,[40,42–52] these

(20) Warren, L. F.; Hawthorne, M. F. *J. Am. Chem. Soc.* **1970**, *92*, 1157–1173.

(21) Dichtel, W. R.; Heath, J. R.; Stoddart, J. F. *Philos. Trans. R. Soc. a−Math. Phys. Eng. Sci.* **2007**, *365*, 1607–1625.

(22) Diehl, M. R.; Steuerman, D. W.; Tseng, H. R.; Vignon, S. A.; Star, A.; Celestre, P. C.; Stoddart, J. F.; Heath, J. R. *ChemPhysChem* **2003**, *4*, 1335–1339.

(23) Kim, H.; Goddard, W. A.; Jang, S. S.; Dichtel, W. R.; Heath, J. R.; Stoddart, J. F. *J. Phys. Chem. A* **2009**, *113*, 2136–2143.

(24) Luo, Y.; Collier, C. P.; Jeppesen, J. O.; Nielsen, K. A.; DeIonno, E.; Ho, G.; Perkins, J.; Tseng, H. R.; Yamamoto, T.; Stoddart, J. F.; Heath, J. R. *ChemPhysChem* **2002**, *3*, 519.

(25) Xue, M.; Kabehie, S.; Stieg, A. Z.; Tkatchouk, E.; Benitez, D.; Stephenson, R. M.; Goddard, W. A.; Zink, J. I.; Wang, K. L. *Appl. Phys. Lett.* **2009**, *95*, 093503−3.

(26) Kabehie, S.; Stieg, A. Z.; Xue, M.; Liong, M.; Wang, K. L.; Zink, J. I. *J. Phys. Chem. Lett.* **2010**, *1*, 589–593.

(27) Piestert, F.; Fetouaki, R.; Bogza, M.; Oeser, T.; Blümel, J. *Chem. Commun.* **2005**, 1481–1483.

(28) Kloster, G. M.; Watton, S. P. *Inorg. Chim. Acta* **2000**, *297*, 156–161.

(29) Terry, T. J.; Stack, T. D. P. *J. Am. Chem. Soc.* **2008**, *130*, 4945–4953.

(30) Schmittel, M.; Michel, C.; Wiegrefe, A. *Synthesis* **2005**, *2005*, 367–373.

(31) Sonogashira, K.; Tohda, Y.; Hagihara, N. *Tetrahedron Lett.* **1975**, *16*, 4467–4470.

(32) Saitoh, Y.; Koizumi, T.-a.; Osakada, K.; Yamamoto, T. *Can. J. Chem.* **1997**, *75*, 1336–1339.

(33) Dominguez, Z.; Dang, H.; Strouse, M. J.; Garcia-Garibay, M. A. *J. Am. Chem. Soc.* **2002**, *124*, 7719–7727.

(34) Ruthkosky, M.; Castellano, F. N.; Meyer, G. J. *Inorg. Chem.* **1996**, *35*, 6406–6412.

(35) Cai, Q.; Luo, Z.-S.; Pang, W.-Q.; Fan, Y.-W.; Chen, X.-H.; Cui, F.-Z. *Chem. Mater.* **2001**, *13*, 258–263.

(36) Sigel, H.; Huber, P. R.; Griesser, R.; Prijs, B. *Inorg. Chem.* **1973**, *12*, 1198–1200.

(37) Sigel, H. *Angew. Chem., Int. Ed. Engl.* **1975**, *14*, 394–402.

(38) Fan, J.; Bats, J. W.; Schmittel, M. *Inorg. Chem.* **2009**, *48*, 6338–6340.

(39) Schmittel, M.; Ganz, A. *Chem. Commun.* **1997**, *999*, 1000.

(40) Schmittel, M. M., C.; Liu, S.-X.; Schildbach, D.; Fenske, D. *Eur. J. Inorg. Chem.* **2001**, 1155–1166.

(41) Malini-Balakrishnan, R.; Scheller, K. H.; Haering, U. K.; Tribolet, R.; Sigel, H. *Inorg. Chem.* **1985**, *24*, 2067–2076.

(42) Kalsani, V.; Schmittel, M.; Listorti, A.; Accorsi, G.; Armaroli, N. *Inorg. Chem.* **2006**, *45*, 2061–2067.

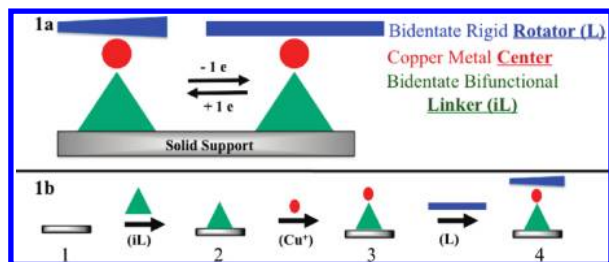(43) Halper, S. R.; Cohen, S. M. *Inorg. Chem.* **2005**, *44*, 4139–4141.

Figure 1. Schematic diagram of the copper switch components. (1a) iL is a bidentate bifunctional linker (triangle) that is covalently immobilized on a solid support, a copper ion is the metal center (circle) that is coordinated to both the linker and the rotator, and L is the bidentate rigid rotator (rectangle). Two states are shown, (1a, upper left) Cu(I) tetrahedral and (1a, upper right) Cu(II) square planar. In the Cu(I) system, the ligands are perpendicular to one another while in the Cu(II) system the ligands are parallel to one another. (1b) The surface-outward sequential synthesis involves: (1) the solid support, (2) the immobilization of the linker, (3) the addition of the copper center, and (4) the addition of the rotator.

interactions prohibit the isomerization of Cu(I) tetrahedral to Cu(II) square planar geometries. For the purpose of using heteroleptic copper compounds as a state variable, at least one ligand needs to be able to rotate freely.

The strategy to synthesize heteroleptic copper compounds with nonhindered ligands that can have a large-amplitude rotational conformational change involves a surface-outward sequential synthesis.[26] The design of heteroleptic copper compounds presented here involves four subunits: (1) a support to serve as a solid-state platform, (2) a bifunctional chelating ligand that is covalently immobilized on the support and can bind to a copper center through bidentate coordination interactions (*linker*), (3) a Cu(I) or Cu(II) metal center, and (4) a bidentate rigid ligand (*rotator*). This method begins with an immobilized ligand (iL, *linker*) on a solid support, with the subsequent addition of copper (Cu$^+$), followed by the chelation of a second ligand (L, *rotator*), shown by eq 1 and illustrated by Figure 1.

$$iL + Cu^+ + L \rightarrow [CuiLL]^+ \qquad (1)$$

Two classes of bidentate ligands were used as the linker (iL): substituted 1,10-phenanthrolines and bisphosphines. Modified 1,10-phenanthroline ligands are an important class of chelating agents[53] and are particularly attractive due to their rigidity, high affinity for metal centers, and ease of modification. Although diimines have one of the highest binding affinities for a copper metal center (e.g., 1,10-phenanthroline: $K_1 = 7 \times 10^8$, $K_2 = 4$

$\times 10^6$, $K_3 = 10^5$),[54] bisphosphine ligands also form favorable bonds to copper.[55]

Multiple linker and rotator components that use these types of ligands were designed and synthesized to allow for versatility in the fabrication of nanodevices (Scheme 2). For example, the designs include a short (~1 nm) rotator that can be used for memory in intramolecular vertical conductance measurements[25] and long (~2 or 3 nm) rigid rotators with long π-conjugated arms that can undergo large-amplitude motion and function as molecular machines. Along similar lines, immobilized linkers (Scheme 3) with an sp^3 center (iS1) or a monosubstituted 1,10-phenanthroline ligand (iS2) allow for flexibility of linker rotation if and when a rotator is prohibited from motion due to the deposition of a top gold electrode via shadow mask evaporation of Si-immobilized heteroleptic copper compounds.[26] In other words, the relative 90° rotational motion of the linker and rotator, with respect to each other, will cause an overall isomerization of the copper compound. S1 is particularly attractive due to its rigidity in standing up on the surface. Additionally, its phosphorus-containing ligands facilitate characterization via solid-state ^{31}P NMR. S2 is useful because it is not easily oxidized chemically when switching between the Cu(I) and Cu(II) SiO$_2$-immobilized systems. S3, a disubstituted 1,10-phenanthroline, has linkers in the 4,7 positions that allow for a more stationary linker that will not rotate about an sp^3 center (a characteristic that is desirable for intermolecular horizontal conductance measurements but not as important for intramolecular conductance measurements).

1. Homoleptic Copper Compounds. Homoleptic copper compounds were prepared as model compounds for the solid-state heteroleptic analogues. The homoleptic copper compound, copper bis-3,8-di(ethynyltrityl)-1,10-phenanthroline (Cu(RM)$_2^+$), is easily synthesized (Figure S14a, Supporting Information). Despite the bulky ethynyltrityl groups present on the 3,8 positions of RM, large-amplitude intra-rotational motion of the bisRM ligands with respect to one another occurs upon oxidation of Cu(I) to Cu(II). This is further supported by the lack of luminescence in Cu(RM)$_2^+$ and(Cu(RL)$_2^+$) as compared to the highly luminescent 2,9-disubstituted aryl groups in homoleptic copper compounds. The luminescence in copper(I) compounds is attributed to the lack of isomerization in Cu(I) to Cu(II) compounds caused by steric bulk.[12–14,42,56,57] In order for the phenanthroline ligands to isomerize with the most efficient conformational change, the long, rigid π-conjugated substituents (e.g., present in ligands RM and RL) need to be on the 3,8 (not the 2,9) positions of 1,10-phenanthroline.

The reduction potentials obtained via cyclic voltammetry for Cu(RM)$_2^{2+/+}$ and Cu(RL)$_2^{2+/+}$ compared to copper bis-1,10-phenanthroline ((Cu(phen)$_2$)$^{2+/+}$) and copper bis-2,9-dimethyl-1,10-phenanthroline ((Cu(RS)$_2$)$^{2+/+}$) are shown in Table 1.[34,57,58] The relatively high Cu(RM)$_2^{2+/+}$ and Cu(RL)$_2^{2+/+}$ couples compared to the Cu(phen))$_2^{2+/+}$ couple can be attributed to the additional electron-donating groups provided by the trityl

(44) Halper, S. R.; Malachowski, M. R.; Delaney, H. M.; Cohen, S. M. *Inorg. Chem.* **2004**, *43*, 1242–1249.

(45) Listorti, A.; Accorsi, G.; Rio, Y.; Armaroli, N.; Moudam, O.; Gegout, A.; Delavaux-Nicot, B.; Holler, M.; Nierengarten, J.-F. O. *Inorg. Chem.* **2008**, *47*, 6254–6261.

(46) Miller, M. T.; Gantzel, P. K.; Karpishin, T. B. *J. Am. Chem. Soc.* **1999**, *121*, 4292–4293.

(47) Pogozhev, D.; Baudron, S. A.; Hosseini, M. W. *Inorg. Chem.* **2009**, *49*, 331–338.

(48) Schmittel, M.; Michel, C.; Wiegrefe, A.; Kalsani, V. *Synthesis* **2001**, *10*, 1561.

(49) Stange, A. F.; Wolfgang, K. *Z. Anorg. Allg. Chem.* **1996**, *622*, 1118–1124.

(50) Cuttell, D. G.; Kuang, S. M.; Fanwick, P. E.; McMillin, D. R.; Walton, R. A. *J. Am. Chem. Soc.* **2002**, *124*, 6–7.

(51) Qin, L.; Zhang, Q. S.; Sun, W.; Wang, J. Y.; Lu, C. Z.; Cheng, Y. X.; Wang, L. X. *Dalton Trans.* **2009**, 9388–9391.

(52) Zhang, Q. S.; Ding, J. Q.; Cheng, Y. X.; Wang, L. X.; Xie, Z. Y.; Jing, X. B.; Wang, F. S. *Adv. Funct. Mater.* **2007**, *17*, 2983–2990.

(53) Sammes, P. G.; Yahioglu, G. *Chem. Soc. Rev.* **1994**, *5*, 327–334.

(54) Jorgensen, C. K. *Inorganic Complexes*; Academic Press Inc.: New York, 1966; Vol. 1.

(55) Black, J. R.; Levason, W.; Spicer, M. D.; Webster, M. *J. Chem. Soc., Dalton Trans.* **1993**, 3129–3136.

(56) Dietrich-Buchecker, C. O.; Marnot, P. A.; Sauvage, J.-P.; Kirchoff, J. R.; McMillin, D. *J. Chem. Soc., Chem. Commun.* **1983**, 513–515.

(57) Eggleston, M. K.; McMillin, D. R.; Koenig, K. S.; Pallenberg, A. J. *Inorg. Chem.* **1997**, *36*, 172–176.

(58) Scaltrito, D. V.; Thompson, D. W.; O'Callaghan, J. A.; Meyer, G. J. *Coord. Chem. Rev.* **2000**, *208*, 243–266.

Scheme 3. Surface-Outward Sequential Synthesis for Selected Heteroleptic Copper Compounds
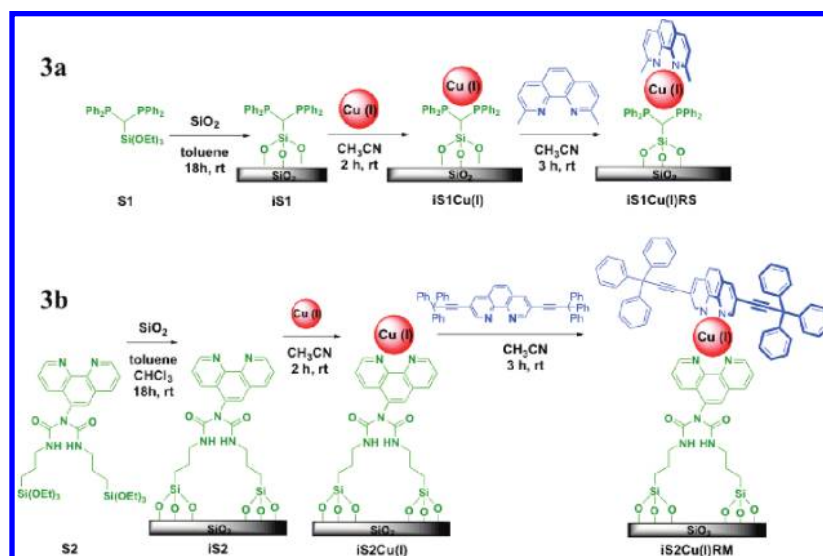
Table 1. Redox Potentials for Cuprous Phenanthroline Derivatives[a]

compound	Cu[II/I] (V)
Cu[I](phen)$_2$[+]	0.54
Cu[I](RM)$_2$[+]	0.84
Cu[I](RL)$_2$[+]	0.92
Cu[I](RS)$_2$[+]	0.99

[a] Measured at room temperature in 0.1 M TBAH/CH$_2$Cl$_2$ vs SCE with ferrocene as an internal standard.

acetylene and 4-ethynylbiphenyl groups from RM and RL, resepectively.[57]

2. Heteroleptic Copper Compounds. A total of six compounds (three linkers and three rotators), shown in Scheme 2, can be used in a modular synthetic approach to synthesize nine combinations of surface-immobilized heteroleptic Cu(I) compounds (or 18 total compounds when Cu(II) analogues are included). Each component allows for the versatility of device fabrication and serves useful purposes in the flexibility of the design. Different combinations of linkers and rotators form assemblies with criterion for through-molecule conductance (intramolecular) or horizontal conductance (intermolecular) device geometries. In other words, through-molecule conductance refers to intramolecular conductance from the top ligand through the metal center to the linker, while horizontal conductance refers to conductance from the π-conjugated top ligand to neighboring π-conjugated top ligands.

Silica nanoparticles were chosen as a model solid support because (1) their surface properties mimic the native oxide layer of silicon, (2) linkers can be covalently attached with high surface area, and (3) their high dispersibility in dimethyl sulfoxide is extremely practical for optical measurements using UV−vis absorption spectroscopy. Solid-state NMR, electron paramagnetic resonance (EPR), and UV−vis absorption studies cannot be carried out using p[+] Si wafers. The commercially available Merck silica is useful for solid-state NMR and EPR characterization, and silica nanoparticles dispersed in liquids are favorable for UV−vis absorption spectroscopy characterization. Silicon is also a favorable support for the linkers shown in Scheme 2 because alkoxysilanes form strong anchors to the native oxide layer on silicon. Additionally, p[+]-doped silicon wafers are useful for conductance measurements when a top electrode (macroscopic gold electrodes via shadow mask

evaporation or a Pt/Ir AFM tip) is used to complete the device assembly.[25,26]

Among the linkers that have been immobilized on a silica support, iS1[27] (Scheme 3a) is attractive due to its short length and phosphorus-containing ligands that have a high isotopic ratio for NMR and hence allow for the easy detection of surface-modified silica particles via solid-state NMR studies. Phosphorus-31 solid-state NMR spectroscopy is a useful tool due to the phosphorus atom's great natural abundance (100%), large chemical shift dispersion with $^1/_2$ spin nucleus, and the improvement in the quality of spectra with magic angle spinning (MAS) and cross-polarization (CP) techniques.[59] On the other hand, iS2[28] (Scheme 3b) is attractive due to its robustness against chemical redox agents and the fact that its absorption spectrum does not interfere with the RM π→π* region (Figures S12 and S13, Supporting Information). Both iS1 and iS2 have flexibility in rotating when placed in a vertical device geometry due to the sp[3] center in iS1 and the monosubstituted 1,10-phenanthroline with an sp[3] center in iS2.[25] iS3 was designed as a disubstituted 1,10-phenanthroline linker that allows full 90° rotation of the upper ligand, since this linker (the bottom ligand) is rigidly immobilized at two points of the molecule. This rigidity is desirable for horizontal conductance measurements in logic applications where alignment is critical.

3. Divergent Synthesis. S1 was immobilized on silica particles to yield the immobilized linker iS1 (Scheme 3a). The ^{13}C CP/MAS solid-state NMR spectrum for iS1 (Figure S4a, Supporting Information) shows two types of carbon peaks associated with iS1. The aromatic region is attributed to the phenyl groups bound to the phosphine. Two peaks appear in the aliphatic region at 59.46 and 16.36 ppm and are attributed to unbound ethoxy[60] groups from iS1, from the methylene and methyl carbon atoms of the ethoxy group, respectively. The appearance of these two residual peaks is known because trialkoxysilane reagents do not exclusively form three siloxane bonds upon condensation reaction with silica surface silanol groups: there always exists a distribution of silane species bound by one, two, and three siloxane bonds.[60] The ^{31}P CP/MAS solid-state NMR spectrum for iS1 shows two peaks at 31.38 and −28.30 ppm. The rotational spin of the sample was 10 kHz, and corresponding

(59) Blümel, J. *Inorg. Chem.* **1994**, *33*, 5050−5056.
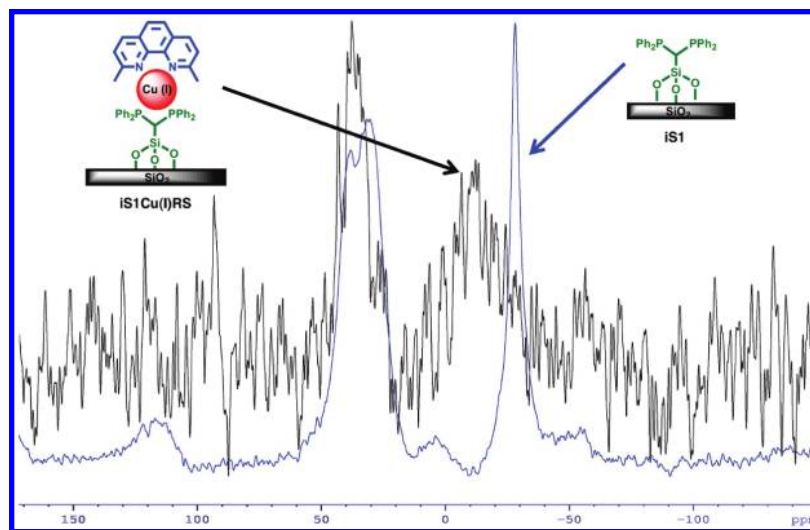(60) Blümel, J. *J. Am. Chem. Soc.* **1995**, *117*, 2112−2113.

Figure 2. ^{31}P CP/MAS solid-state NMR of iS1 and iS1Cu(I)RS.

spinning sidebands are observed. The peak at 31.38 ppm is from the formation of a phosphine–oxide with the surface (Figure S4b).[59,61] This is confirmed by addition of hydrogen peroxide to iS1, where it is observed that the peak at −28.30 ppm has been oxidized (Figure S4c) to the peak at 31.38 ppm.

S2 was also immobilized on silica, and the ^{13}C CP/MAS solid-state NMR spectrum of iS2 (Scheme 3b) shows carbon atom peaks in the carbonyl, aromatic, and aliphatic regions (Figure S5a, Supporting Information). Similar to iS1, the ^{13}C CP/MAS solid-state NMR of iS2 contains residual alkoxide signals at 59.22 and 16.96 ppm from unbound ethoxy groups. In addition, a methanol wash of iS2 results in a methoxide peak that appears at 50.46 ppm. ^{29}Si CP/MAS solid-state NMR confirms the covalent bonding that forms between S2 and the silica particles (Figure S5b). The peaks corresponding to the various siloxane Q^m and organosiloxane T^n species can be identified clearly.[62] The T^n bands [$T^n = RSi(OSi)_nOH_{3−n}$, $n = 1−3$] are resonances of the Si to which the linkers are bonded, whereas the Q^m bands [$Q^m = Si(OSi)_m(OH)_{4−m}$, $m = 2−4$] correspond to bulk and surface Si to which only oxygen atoms are bonded.

The immobilized ligand, iS3, was produced by the immobilization of S3 on the solid silica support. The ^{13}C CP/MAS solid-state NMR spectrum of iS3 confirms the presence of aromatic and aliphatic carbon atoms (Figure S6a, Supporting Information) in addition to the residual ethoxide signals. The ^{29}Si CP/MAS solid-state NMR spectrum shows the T and Q regions of the silicon atoms. The T region shows the binding of one, two, and three ethoxy groups to the solid silica support (Figure S6b).

Following the divergent synthetic scheme, subsequent attachment of the metal center and rotator is carried out. In a typical synthesis, copper(I) tetrakis(acetonitrile)hexafluorophosphate was chosen as the starting oxidation state for the copper metal center because of its high solubility in organic solvents such as acetonitrile and methylene chloride. In the case of iS1, starting independently with both Cu(I) and Cu(II) was necessary since the phosphine atoms in iS1 oxidize in the presence of oxidizing agents.[59,61] In other words, chemical redox

(61) Sommer, J.; Yang, Y.; Rambow, D.; Blümel, J. *Inorg. Chem.* **2004**, *43*, 7561–7563.
(62) Peng, C.; Zhang, H.; Yu, J.; Meng, Q.; Fu, L.; Li, H.; Sun, L.; Guo, X. *J. Phys. Chem. B* **2005**, *109*, 15278–15287.

agents cannot be used to demonstrate the reversible two states of the Cu(I) and Cu(II) analogues in the presence of iS1.

The rotators are relatively *short* (RS, ∼1 nm), *medium* (RM, ∼2 nm), and *long* (RL, ∼3 nm) in size. RS is commercially available, while RM and RL were synthesized by the Sonogashira coupling of 3,8-dibromo-1,10-phenanthroline to tritylacetylene and 4-ethynylbiphenyl, respectively.

4. Properties of iS1Cu(I)RS. To illustrate the properties of compounds prepared by divergent syntheses and described in the previous section, iS1Cu(I)RS is an example of a compound where the first linker and shortest rotator are examined. Addition of Cu(I) and RS to iS1 yields the compound iS1Cu(I)RS. The ^{31}P CP/MAS solid-state NMR spectrum for iS1Cu(I)RS shows the shift of the iS1 ^{31}P CP/MAS solid-state NMR signal from −28.30 to −12.15 ppm. This confirms the complexation of Cu(I) to iS1 (Figure 2).[55] The signal in the ^{13}C CP/MAS solid-state NMR spectrum of the aromatic carbon atoms from the phenanthroline portion of RS overlaps with the aromatic carbon atom signals from the phenyl groups on the phosphorus atoms in iS1. However, the methyl carbons on the 2,9 positions of the phenanthroline ligand of RS are distinctly observed in the ^{13}C CP/MAS solid-state NMR spectrum of iS1Cu(I)RS and appear at 23.81 ppm. Although this signal is broad enough to interfere with the methylene carbon atom in iS1, a comparison of the ^{13}C CP/MAS spectra of iS1 and iS1Cu(I)RS shows the distinction when RS is added to the compound (Figure S9b, Supporting Information).

Overall, although the number of scans of the iS1Cu(I)RS ^{13}C and ^{31}P CP/MAS solid-state NMR spectra is greater than that of the iS1 ^{13}C and ^{31}P CP/MAS solid-state NMR spectra, the signal-to-noise for iS1Cu(I)RS is significantly worse. This is a consequence of the presence of a small amount of Cu(II) on the silica surface. The paramagnetic nature of Cu(II) vs Cu(I) significantly decreases the S/N ratio of the spectra (Figure S9a). EPR was used to confirm the presence of Cu(II) on the silica support (Figure S9c). Additionally, UV–vis absorption spectra of independently synthesized iS1Cu(I)RS and iS1Cu(II)RS show that a metal-to-ligand charge-transfer (MLCT) band is present for the Cu(I) species, indicative of the tetrahedral geometry. However, no MLCT band is present for the iS1Cu(II)RS, implying a different geometry (i.e., square planar) from the Cu(I) form (Figure 3).
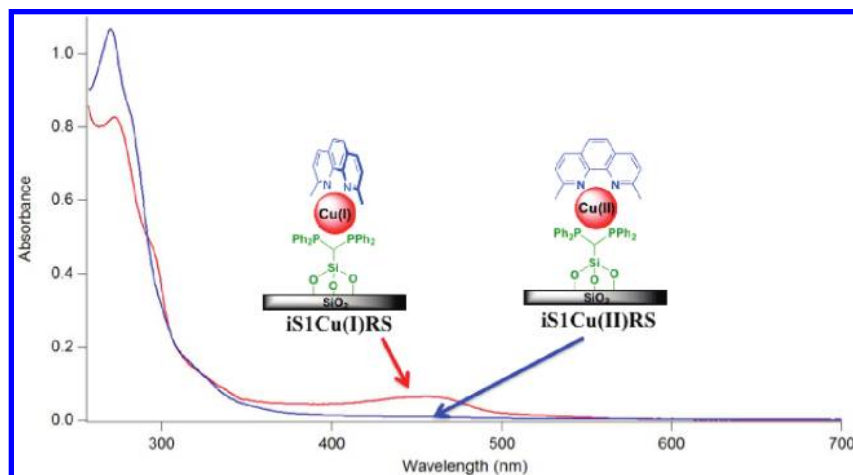
Figure 3. An amount of 2.5 mL of the particle suspension (100 µg/mL) in DMSO of independently synthesized iS1Cu(I)RS and iS1Cu(II)RS. The Cu(I) form has a MLCT around 450 nm, but the Cu(II) form does not. The red curve represents the reduced state, while the blue curve represents the oxidized state.

5. Properties of iS2Cu(I)RS and iS2Cu(I)RM. To illustrate the properties of compounds prepared by divergent synthesis, iS2Cu(I)RS and iS2Cu(I)RM are examples of compounds examined where the second linker is used with either the shortest rotator or a medium-length rotator, respectively. The addition of Cu(I) and RS to iS2 produces iS2Cu(I)RS (Scheme 3b). Unlike iS1Cu(I)RS, the methyl groups from the 2,9 position of the phenanthroline ring of RS are not clearly observed in the ^{13}C CP/MAS solid-state NMR spectrum of iS2Cu(I)RS because the signal interferes with the aliphatic carbons of iS2 (Figure S10a,b, Supporting Information). Therefore, the subsequent addition of Cu(I) and RM to produce iS2RM was used to distinguish between the carbon atom signals of iS2 and RM. The ^{13}C CP/MAS solid-state NMR spectrum of RM shows additional carbon signals that result from the tritylacetylene groups of the phenanthroline ring present on the 3,8 positions of RM. The acetylene group contributes to carbon signals at 99.16 and 81.73 ppm, while the trityl carbon results in a carbon atom signal at 56.38 ppm (Figure S7b, Supporting Information). Comparison of the ^{13}C CP/MAS solid-state NMR spectra of iS2 and iS2Cu(I)RM shows the addition of RM to iS2 and Cu(I) (Figure S11c, Supporting Information). Like iS1Cu(I)RS, the poor S/N ratio in the solid-state NMR spectra of iS2Cu(I)RS and iS2Cu(I)RM shows the presence of paramagnetic Cu(II). This presence is confirmed via EPR (Figures S10c and S11d). It is noteworthy that, over time, the slow oxidation of Cu(I) to Cu(II) occurs. Therefore, the addition of a reducing agent, such as ascorbic acid, to the immobilized Cu(I) compounds returns air-oxidized Cu(II) centers back to Cu(I).

The absorption spectra after adding ascorbic acid shows that any remaining Cu(II) was reduced to Cu(I), and hence an increase of the MLCT band at ~450 nm was observed (Figure S11e). UV−vis absorption spectroscopy was also used to distinguish between iS2Cu(I)RS and iS2Cu(I)RM immobilized on silica nanoparticles and dispersed in dimethyl sulfoxide (DMSO) (Figure S11f). iS2Cu(I)RS and iS2Cu(I)RM can be distinguished by the additional shoulder at ~336 nm in the iS2Cu(I)RM spectrum. This peak is attributed to the RM ligand of iS2Cu(I)RM. The UV−vis absorption of iS2Cu(I)RS and iS2Cu(I)RM is compared to that of their Cu(II) analogues that were formed by the oxidizing agent, hydrogen peroxide (Figure 4).

6. Heteroleptic Copper Switches. The switching properties of the SiO$_2$- and p$^+$ Si-immobilized heteroleptic copper com-

pounds were studied. The switching characteristics of the SiO$_2$-immobilized systems were explored via chemical redox agents, UV−vis absorption spectroscopy, and EPR. The p$^+$ Si-immobilized heteroleptic copper switches were studied by two methods: (1) macroscopic gold electrodes[25] and (2) a cAFM tip.[26]

7. Heteroleptic Copper Switches on Silica Nanoparticles Using Chemical Redox Agents. Tetravalent copper compounds are known to exhibit different geometries based on the charge of the copper metal center and the absence of sterically hindering substituents on the 2,9 positions of 1,10-phenanthroline. More specifically, copper(I) bis-bidentate compounds are tetrahedral, while the copper(II) analogues are generally square planar.[10,63] Hence, up to a 90° rotation of the ligands, with respect to one another, can be achieved via oxidation and reduction of the copper metal center.

Absorption spectra of iS2Cu(I)RS, iS2Cu(I)RM, iS3Cu(I)RS, and iS3Cu(I)RM were measured by suspending the modified silica nanoparticles in DMSO. The MLCT band in all four samples appears at ~450 nm. Upon the addition of hydrogen peroxide and then washing of the particles, all four samples were separately oxidized to Cu(II) compounds. The presence of Cu(II) was observed by the disappearance of the MLCT. These samples were subsequently reduced back to Cu(I) by the addition of ascorbic acid followed by a wash. The MLCT band reappeared upon the reduction of Cu(II) to Cu(I) (Figures S10d, S11e, S12, S13, Supporting Information).

EPR characterization is a powerful tool used to determine the structure of paramagnetic compounds, including but not limited to Cu(II) compounds.[64,65] Additional data that support the isomerization of Cu(I) tetrahedral to Cu(II) square planar are extracted from EPR data. To begin with, the bis(1,10-phenanthroline) Cu(I) compounds are known to be tetrahedral[66] (Figure S14a, Supporting Information), while Cu(II) analogues are square planar.[63] Based on the MLCT band at ~450 nm for the heteroleptic copper compounds discussed above (iS1Cu(II)RS, iS2Cu(II)RS, and iS2Cu(II)RM) and the crystal structure from Figure S14a, the SiO$_2$-immobilized heteroleptic copper compounds are considered to be tetrahedrally shaped. Upon oxidation of the Cu(I) center, isomerization of Cu(II) square planar takes place, and this structural change is confirmed on the basis
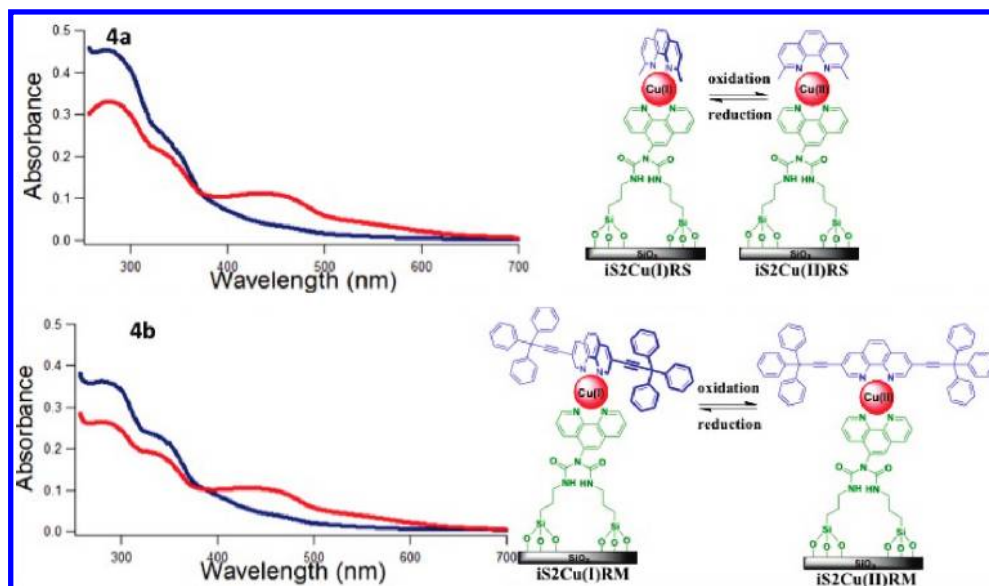
Figure 4. An amount of 2.5 mL of the particle suspension (100 μg/mL) in DMSO of (a) iS2Cu(I)RS and (b) iS2Cu(I)RM, where the red-curves represent the reduced state. Disappearance of the MLCT band of Cu(I) ($\sim$450 nm) is observed upon use of an oxidizing agent, H_2O_2, where the blue curves represent the oxidized state.
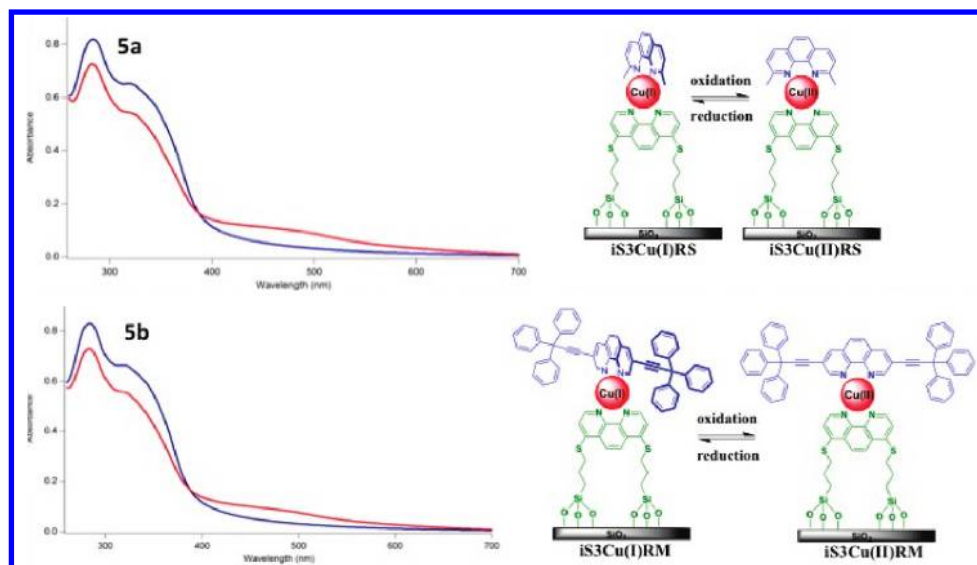

Figure 5. An amount of 2.5 mL of the particle suspension (100 μg/mL) in DMSO of (a) iS3Cu(I)RS and (b) iS3Cu(I)RM, where the red curves represent the reduced state. Disappearance of MLCT band of Cu(I) ($\sim$ 450 nm) is observed upon use of an oxidizing agent, H_2O_2, where the blue curves represent the oxidized state. The absorption spectrum of iS3 interferes with the $\pi \rightarrow \pi*$ transition of RM; hence, iS3Cu(I)RS and iS3Cu(I)RM absorption spectra cannot be distinguished.

of the pattern of the EPR signals shown in Figures S9c, S10c, and S11d (Supporting Information).[64,65]

8. Current−Voltage Spectroscopy of iS1, iS1Cu, and iS1CuRS on p$^+$ Si Using Two Methods. Characterization of switching events in electrical devices can be readily carried out through $I-V$ spectroscopy. Electrical properties of the immobilized molecular monolayers represented in steps 2−4 of Figure 1b were examined in a sandwich-type device architecture at both the macro- and nanoscale through the use of macroscopic

(63) Amournjarusiri, K.; Hathaway, B. J. *Acta Crystallogr., Sect. C* **1991**, *47*, 1383−1385.
(64) Zink, J. I.; Drago, R. S. *J. Am. Chem. Soc.* **1972**, *94*, 4550−4554.
(65) Hyde, J. S.; Pasenkiewicz-Gierula, M.; Basosi, R.; Froncisz, W.; Antholine, W. E. *J. Magn. Reson.* **1989**, *82*, 63−75.
(66) Pallenberg, A. J.; Marschner, T. M.; Barnhart, D. M. *Polyhedron* **1997**, *16*, 2711−2719.
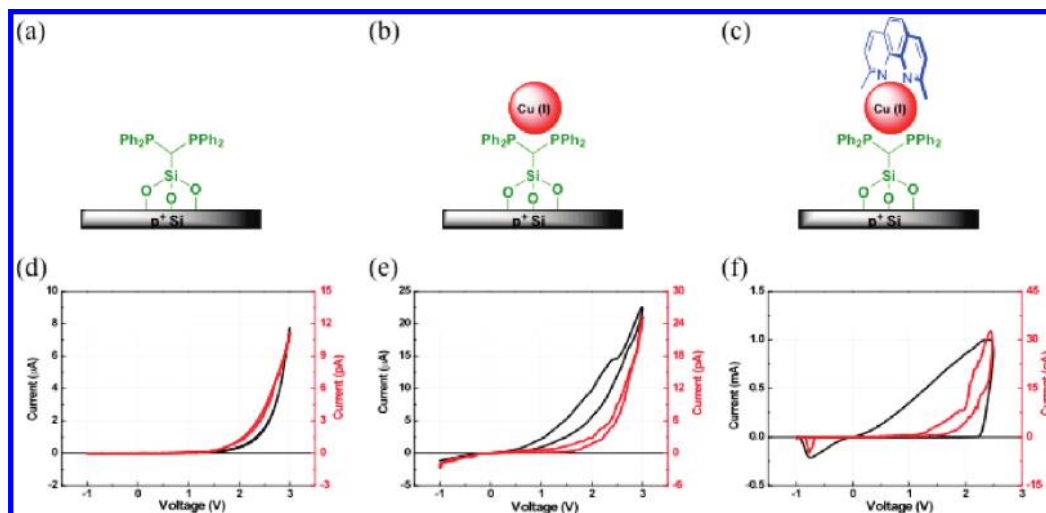
Ti/gold electrodes and localized cAFM, respectively.[1] Discrete switching events are commonly associated with the observation of a distinct increase in conductance above specific threshold voltages in both the positive and negative directions, a persistent ON state current following a switching event, and/or a hysteresis within the acquired $I-V$ curve. As seen in Figure 6, $I-V$ characteristics of devices whose molecular layer consisted of solely grafted linkers (iS1), Cu-ligated linkers (iS1Cu), and the fully formed heteroleptic Cu switch (iS1CuRS) were investigated in order to assess the source of observed solution-phase switching events. Beginning with a device residing in the OFF state, denoted by a lack of measured electrical current, bias voltage sweeps were applied to both iS1 and iS1Cu and resulted in the $I-V$ curves seen in Figure 6d,e. As expected, neither molecular device revealed any of the effects indicating

Figure 6. Schematic diagram of the p$^+$ Si-immobilized heteroleptic copper switch components (a–c) and corresponding *I*–*V* curves acquired on each component layer in using both macroscopic Ti/Au (black) and Pt–Ir cAFM (red) electrodes (d–f), where molecular switching events are solely evident in the fully formed compound (f).

a molecular switching event described above. The lack of a ligated rigid rotator in these devices serves to eliminate any capability for intramolecular rotational motion. *I*–*V* curves acquired on iS1CuRS demonstrated that application of a positive bias >2.2 V produced a drastic increase in conductivity that persisted upon sweeping the bias toward a negative potential, as seen in Figure 6f. Application of a bias greater than −1 V caused the ON state to be switched OFF and generated a corresponding, abrupt decrease in conductivity that persisted until the positive threshold voltage was applied. In combination, these results indicate that observed switching effects in fully formed molecular devices are the result of conformational effects and do not stem from either the ligand subunits themselves or the interfaces between the ligands and the metal electrodes.

Summary

The design and synthesis of a library of silica-immobilized heteroleptic copper compounds was reported. The method used to compose this library of heteroleptic compounds involved surface-outward sequential synthesis. A modular synthetic approach of three individual components comprised this class of functional materials and included a (1) bidentate linker immobilized on silica, (2) a Cu(I) or Cu(II) metal center, and (3) a rigid and bidentate rotator. Solid-state NMR, EPR, and UV–vis absorption spectroscopies were used to characterize these silica-immobilized heteroleptic copper compounds. Hydrogen peroxide and ascorbic acid were used as chemical redox agents to change the oxidation state of the heteroleptic copper compounds from Cu(I) to Cu(II) and then back to Cu(I). Optical spectroscopy of a DMSO suspension demonstrated the reversibility of the Cu(I)/Cu(II)-immobilized compounds by monitoring the disappearance and appearance of the MLCT band at 450 nm. EPR spectroscopy confirmed the structure of the SiO$_2$-immobilized Cu(II) species as square planar. The electrical properties of these heteroleptic copper compounds immobilized on p$^+$ Si, as determined using macroscopic gold electrodes[25]

and cAFM,[26] make these materials promising candidates for future memory and logic applications.

Experimental Section

1. Linkers. [Bis(diphenylphosphino)methyl]triethoxysilane (S1).[27] A solution of bis(diphenylphosphino)methane (1.02 g, 2.60 mmol) in 15 mL of toluene was treated with 1.62 mL (2.60 mmol) of 1.6 M n-BuLi in hexane and allowed to stir under an N$_2$ atmosphere at room temperature. After 6 h, 0.511 mL (2.60 mmol) of chlorotriethoxysilane was added dropwise under rapid stirring. After complete addition, the reaction mixture was stirred for an additional 30 min. Toluene was removed by vacuum evaporation, and the reaction mixture was dissolved in pentane. Centrifugation was used to separate the lithium salt, and the supernatant was dried in vacuo to remove the pentane to yield 67% of product (0.824 g, 1.51 mmol). ^{1}H NMR (500 MHz, C$_6$D$_6$): δ 7.99–7.36 (m, 8 H), 7.09–6.89 (m, 12 H), 3.95 (q, 6H), 2.79 (s, 1H), 1.22 (t, 9H). ^{31}P NMR (202 MHz, C$_6$D$_6$): δ −21.12.

5-*N*,*N*-Di(amidopropyltriethoxysilane)-1,10-phenanthroline (S2).[28] A total of 0.200 g (1.02 mmol) of 5-amino-1,10-phenanthroline was dissolved in 30 mL of CHCl$_3$ and filtered into a reaction flask. The solution was stirred while 1.6 mL (∼ 6.5 mmol) of 3-(triethoxysilyl)propyl isocyanate was added. The chloroform was evaporated at atmospheric pressure, and the resulting mixture was heated at 80 °C, under N$_2$, overnight. The reaction mixture was allowed to reach room temperature and was then placed in an ice bath. Cold hexanes were added to precipitate an off-white powder. Centrifugation, decanting of the supernatant, and then dissolution of the solid in methanol were carried out. The solution was gravity filtered, the methanol was then removed by rotary evaporation, and the final product was dried under vacuum overnight to yield 0.274 g, 0.397 mmol (39%). ^{1}H NMR (500 MHz, CDCl$_3$): δ 9.22 (m, 2H), 8.29 (m, 2H), 7.89 (s, 1H), 7.71 (m, 2H), 3.70 (q, 12H), 3.23 (m, 4H), 2.10 (br, 2H), 1.60 (m, 4H), 1.13 (t, 18H), 0.53 (m, 4H).

4,7-Di(3-(triethoxysilyl)propylthio)-1,10-phenanthroline (S3).[29] 4,7-Dichloro-1,10-phenanthroline (200 mg, 0.803 mmol) was stirred with 20 equiv of 3-mercaptopropyltriethoxysilane (4.13 mL, 16.1 mmol) and 40 equiv of K$_2$CO$_3$ (4.44 g, 32.1 mmol, dried in oven overnight) in anhydrous THF under N$_2$ for 36 h at 65 °C. The mixture was cooled and centrifuged, and the THF from the supernatant was removed under vacuum to give a green oil. Dissolution of the oil in pentane followed by cooling to −115 °C precipitated the final product in a pure form (72% yield, 378 mg,

0.578 mmol). ^{1}H NMR (500 MHz, CDCl$_3$): δ 9.56 (d, J = 4.7 Hz, 2H), 8.55 (s, 2H), 8.12 (d, J = 4.3 Hz, 2H), 3.82 (q, J = 7.0 Hz, 12 H), 2.70 (t, J = 7.0 Hz, 4H), 1.81 (m, 4H), 1.23 (t, J = 7.0 Hz, 18 H), 0.73 (t, J = 8.3 Hz, 4H). MS (ESI): calcd for C$_{30}$H$_{49}$N$_2$O$_6$S$_2$Si$_2$ [M + H]$^+$ 653.26, found 653.24.

2. Immobilization of Linkers. iS1, iS2, and iS3. A total of 0.3 g of silica was slurried in about 50 mL of toluene, and excess S1 (3 × 10^{-4} mol dissolved in 4 mL of toluene), S2 (3 × 10^{-4} mol dissolved in 4 mL of CHCl$_3$), or S3 (3 × 10^{-4} mol dissolved in 4 mL of THF) was added. The reaction mixture was stirred for 18 h, under N$_2$, at ambient temperature. The reaction mixture was centrifuged, and the supernatant was removed. The modified silica particles were washed three times with toluene and dried overnight under vacuum.

3. Rotators. 3,8-Di(ethynyltrityl)-1,10-phenanthroline (RM). RM was prepared on the basis of modified procedures.[30,31] A mixture of 3,8-dibromo-1,10-phenanthroline[32] (0.54 g, 1.60 mmol, 1 equiv), 3,3,3-triphenylpropyne[33] (2.58 g, 9.60 mmol, 6 equiv), dichlorobis(triphenylphosphine)palladium(II) (0.071 g, 100 μmol), copper iodide (7.6 mg, 0.400 mmol), and anhydrous triethylamine (3.4 mL) was suspended in anhydrous benzene (20 mL). After the mixture was refluxed for 4 d under Ar, the solvent was evaporated. The black residue was dissolved in dichloromethane (150 mL), washed with 2% KCN solution (100 mL) and water (100 mL), and dried over MgSO$_4$. The residue was purified by column chromatography by first dry-loading the crude product with silica, flushing out 3,3,3-triphenylphosphine (hexanes, R_f = 1), and then gradually increasing the polarity of the elute (9:1, 6:1, 3:1, 1:1 hexanes/EtOAc, respectively, and then EtOAc, R_f = 0.16). The product was recrystallized from EtOAc/hexanes. Yield: 0.890 g (1.25 mmol, 78%) of a colorless solid, mp 269 °C. IR (neat): ν_{max} 3086, 3058, 3024, 2218, 1597, 1539, 1490, 1446, 1421 cm^{-1}. ^{1}H NMR (300 MHz, CDCl$_3$): δ 9.24 (d, J = 2.0 Hz, 2H), 8.36 (d, J = 2.0 Hz, 2H), 7.77 (s, 2H), 7.37−7.29 (m, 30H). ^{13}C (125 MHz), CP/MAS: δ 153, 146, 143, 129, 120, 99, 82, 56. MS (ESI): calcd for C$_{54}$H$_{37}$N$_2$ [M + H]$^+$ 713.29, found 713.28.

3,8-Di(4-ethynylbiphenyl)-1,10-phenanthroline (RL). RL was prepared on the basis of modified procedures.[30,31] A mixture of 3,8-dibromo-1,10-phenanthroline (0.54 g, 1.60 mmol, 1 equiv), 4-ethynylbiphenyl (0.627 g, 3.52 mmol, 2.2 equiv), dichlorobis(triphenylphosphine)palladium(II) (0.056 g, 0.08 mmol, ∼10%), copper iodide (0.3 g, 0.16 mmol), and anhydrous triethylamine (10 mL) was suspended in anhydrous benzene (20 mL). After the mixture was refluxed for 1 d under Ar, the solvent was evaporated. The black residue was dissolved in dichloromethane (150 mL), washed with 2% KCN solution (100 mL) and water (100 mL), and dried over MgSO$_4$. The residue was purified by column chromatography by first dry-loading the crude product with silica, flushing out 4-ethynylbiphenyl (SiO$_2$, hexanes, R_f = 1), and then gradually increasing the polarity of the elute (9:1, 6:1, 3:1, 1:1 hexanes/EtOAc, respectively, EtOAc, and then CHCl$_3$, R_f (10% MeOH in EtOAc, 0.1% NEt$_3$) = 0.5). The product was recrystallized from 1,1,2,2-tetrachloroethane with slow diffusion of ether. Yield: 0.605 g (1.14 mmol, 62%) of a pale yellow solid, mp 246−248 °C. IR (neat): ν_{max} 3406, 2920, 2208, 1595, 1522, 1485, 1419 cm^{-1}. ^{1}H NMR (500 MHz, (CD$_3$)$_2$SO): δ 9.28 (d, J = 1.9 Hz, 2H), 8.81 (d, J = 1.9 Hz, 2H), 8.11 (s, 2H), 7.85−7.76 (m, 18H). MS (ESI): calcd for C$_{40}$H$_{25}$N$_2$ [M + H]$^+$ 533.20, found 533.20.

4. Assembly of SiO$_2$-Immobilized Heteroleptic Cu Compounds. In a typical synthesis, 0.2 g of iS1, iS2, or iS3 is slurried in about 30 mL of toluene (see Supporting Information). A concentration of 2 × 10^{-4} mol of [Cu(I)(CH$_3$CN)$_4$]PF$_6$ in 4 mL of CH$_3$CN was added. The reaction mixture was allowed to stir for 2 h, under N$_2$, at ambient temperature. A concentration of 2 × 10^{-4} mol of a RS, RM, or RL in 4 mL of CH$_3$CN, CH$_2$Cl$_2$, or tetrachloroethane, respectively (see Supporting Information), was added to the reaction mixture and was allowed to stir for an additional 3 h. The reaction mixture was centrifuged, and the supernatant was removed. The

modified silica particles were washed three times and dried overnight under vacuum.

5. Homoleptic Cu Species for Crystallography and Electrochemistry. [Cu(I) Bis(3,8-di(ethynyltrityl)-1,10-phenanthroline)]PF$_6$ ([Cu(I)bisRM]PF$_6$). [Cu(I)bisRM]PF$_6$ was prepared on the basis of a previously reported procedure.[34] Two equivalents of RM (7.22 mg, 1 × 10^{-5} mol) was dissolved in 5 mL of CH$_2$Cl$_2$, and the resultant solution was deaerated with argon. To this solution was added, with stirring, 1.9 mg (5 × 10^{-6} mol) of Cu(CH$_3$CN)$_4$(PF$_6$) in 3 mL of CH$_3$CN under an argon atmosphere. An orange-red color was immediately observed, and the reaction mixture was allowed to stir at ambient temperature for 1 h. Next, 35 mL of argon-saturated diethyl ether was added to the reaction mixture. After 3 h, an additional 20 mL of argon-saturated diethyl ether was added to the reaction mixture and allowed to stir overnight under an argon atmosphere. The formed precipitate was filtered onto a glass frit and redissolved in a minimum amount of CH$_2$Cl$_2$. Slow evaporation of diethyl ether produced air-stable crystals of the product in ∼88% yield. MS (MALDI) calcd for C$_{108}$H$_{72}$CuN$_4$ 1488.51, found 1487.98.

[Cu(I) Bis(3,8-di(ethynylbiphenyl)-1,10-phenanthroline)]PF$_6$ ([Cu(I)bisRL]PF$_6$). Two equivalents of RL (5.33 mg, 1 × 10^{-5} mol) was dissolved in 5 mL of tetrachloroethane, and the resultant solution was deaerated with argon. To this solution was added, with stirring, 1.9 mg (5 × 10^{-6} mol) of Cu(CH$_3$CN)$_4$(PF$_6$) in 3 mL of CH$_3$CN under an argon atmosphere. An orange-yellow color was immediately observed, and the reaction mixture was allowed to stir at ambient temperature for 1 h. Next, 35 mL of argon-saturated diethyl ether was added to the reaction mixture and allowed to stir overnight under an argon atmosphere. The formed precipitate was filtered onto a glass frit. ^{1}H NMR (500 MHz, CD$_2$Cl$_2$): δ 7.89−6.79 (m, 46H).

6. UV−Vis Absorption Measurements. Silica nanoparticles were synthesized[35] then functionalized by the copper compound (described in Supporting Information). A total of 2.5 mL of the particle suspension (100 μg/mL) in DMSO was used. Either ascorbic acid or hydrogen peroxide solution was added into the suspension to reduce or oxidize the copper compounds bound on the particle surface, respectively. After the addition of the redox reagent, the particles were washed with and resuspended in DMSO to measure absorbance.

7. Assembly of p$^+$ Si-Immobilized Heteroleptic Cu Compounds. A p$^+$ Si wafer was first washed with a piranha solution (1 part 30% H$_2$O$_2$ and 3 parts H$_2$SO$_4$) and then an aqua regia solution (1:3 HNO$_3$:HCl). The wafer was then immersed into a 1 × 10^{-5} M solution of iS1 (in toluene), iS2 (CHCl$_3$/toluene), or iS3 (THF/toluene) inside a test tube. The test tube was equipped with a stir bar and sealed under an N$_2$ atmosphere. The wafer remained in this stirred solution at ambient temperature, under N$_2$, for approximately 18 h. After excess iS1, iS2, or iS3 was washed away with toluene, acetonitrile, or THF, respectively, the modified wafer containing immobilized linkers was subsequently immersed into a test tube containing a 1 × 10^{-5} M solution of propylaminotriethoxysilane (PTS), equipped with a stir bar, under an N$_2$ atmosphere, at room temperature for an additional 18 h. The wafer was washed with toluene to remove excess PTS, placed in a test tube containing a 1 × 10^{-5} M solution of Cu(I)(CH$_3$CN)$_4$PF$_6$ in CH$_3$CN, under an N$_2$ atmosphere, and then stirred at ambient temperature for 3 h. A concentration of 1 × 10^{-5} M dmp in CH$_3$CN was added to the reaction test tube, and the immersed wafer was allowed to stir under ambient conditions and under an N$_2$ atmosphere for an additional 2 h. The wafer was washed thoroughly with CH$_3$CN, dried with a flow of N$_2$ gas, and then placed in a vacuum desiccator overnight.

8. Electrical Characterization. Electrical properties of the p$^+$ Si-immobilized molecular layers were investigated through current−voltage (I−V) spectroscopy in ambient conditions at both the micro- and nanoscale. First, microscale devices were fabricated by deposition of a Ti/gold film through a shadow mask onto the surface of the molecular layer to form a top electrode. Electrical contact to the device was made using a probe station. Bias voltage

sweeps were applied to the top gold electrode with respect to the grounded p$^+$ Si substrate and analyzed by using a Keithley 4200 semiconductor characterization system. In order to average the nonuniformity of the molecular monolayer, sweep delay and hold times were optimized and resulted in individual measurements requiring 10 min to complete, depending on the measured current level. Second, local nanoscale $I-V$ spectroscopic analyses were carried out via cAFM using the Nanoscope V Dimension Icon instrument (Veeco Instruments). Pt−Ir-coated silicon cantilevers (ContPt, NanoWorld) with calibrated spring constants between 0.12 and 0.15 N/m, first longitudinal resonance frequencies between 11.5 and 13 kHz, and nominal tip radii of <25 nm were employed in contact mode under a minimum constant applied load in order to reduce sample perturbation during the measurement. Bias voltage sweeps were applied to the sample with respect to a virtually grounded cAFM probe tip at a rate of 0.25 V/s over the range of interest. Each point within the bias sweep was sampled five times and averaged to enhance the S/N ratio. Presented $I-V$ curves are composed of a single sweep. While small fluctuations attributed to nonuniformity in the active molecular layer were observed between individual devices, $I-V$ characteristics were stable with repeated positive and negative bias sweeps.

Supporting Information Available: Spectral characterization data. This material is free of charge via the Internet at http://pubs.acs.org.

JA103937V